Measurement of branching fraction of $D_s^{*+} \to D_s^+ \pi^0$ relative to $D_s^{*+} \to D_s^+ \gamma$

M. Ablikim,[1] M. N. Achasov,[11,b] P. Adlarson,[70] M. Albrecht,[4] R. Aliberti,[31] A. Amoroso,[69a,69c] M. R. An,[35] Q. An,[66,53] X. H. Bai,[61] Y. Bai,[52] O. Bakina,[32] R. Baldini Ferroli,[26a] I. Balossino,[27a] Y. Ban,[42,g] V. Batozskaya,[1,40] D. Becker,[31] K. Begzsuren,[29] N. Berger,[31] M. Bertani,[26a] D. Bettoni,[27a] F. Bianchi,[69a,69c] J. Bloms,[63] A. Bortone,[69a,69c] I. Boyko,[32] R. A. Briere,[5] A. Brueggemann,[63] H. Cai,[71] X. Cai,[1,53] A. Calcaterra,[26a] G. F. Cao,[1,58] N. Cao,[1,58] S. A. Cetin,[57a] J. F. Chang,[1,53] W. L. Chang,[1,58] G. Chelkov,[32,a] C. Chen,[39] Chao Chen,[50] G. Chen,[1] H. S. Chen,[1,58] M. L. Chen,[1,53] S. J. Chen,[38] S. M. Chen,[56] T. Chen,[1] X. R. Chen,[28,58] X. T. Chen,[1] Y. B. Chen,[1,53] Z. J. Chen,[23,h] W. S. Cheng,[69c] S. K. Choi,[50] X. Chu,[39] G. Cibinetto,[27a] F. Cossio,[69c] J. J. Cui,[45] H. L. Dai,[1,53] J. P. Dai,[73] A. Dbeyssi,[17] R. E. de Boer,[4] D. Dedovich,[32] Z. Y. Deng,[1] A. Denig,[31] I. Denysenko,[32] M. Destefanis,[69a,69c] F. De Mori,[69a,69c] Y. Ding,[36] J. Dong,[1,53] L. Y. Dong,[1,58] M. Y. Dong,[1,53,58] X. Dong,[71] S. X. Du,[75] P. Egorov,[32,a] Y. L. Fan,[71] J. Fang,[1,53] S. S. Fang,[1,58] W. X. Fang,[1] Y. Fang,[1] R. Farinelli,[27a] L. Fava,[69b,69c] F. Feldbauer,[4] G. Felici,[26a] C. Q. Feng,[66,53] J. H. Feng,[54] K. Fischer,[64] M. Fritsch,[4] C. Fritzsch,[63] C. D. Fu,[1] H. Gao,[58] Y. N. Gao,[42,g] Yang Gao,[66,53] S. Garbolino,[69c] I. Garzia,[27a,27b] P. T. Ge,[71] Z. W. Ge,[38] C. Geng,[54] E. M. Gersabeck,[62] A. Gilman,[64] K. Goetzen,[12] L. Gong,[36] W. X. Gong,[1,53] W. Gradl,[31] M. Greco,[69a,69c] L. M. Gu,[38] M. H. Gu,[1,53] Y. T. Gu,[14] C. Y. Guan,[1,58] A. Q. Guo,[28,58] L. B. Guo,[37] R. P. Guo,[44] Y. P. Guo,[10,f] A. Guskov,[32,a] T. T. Han,[45] W. Y. Han,[35] X. Q. Hao,[18] F. A. Harris,[60] K. K. He,[50] K. L. He,[1,58] F. H. Heinsius,[4] C. H. Heinz,[31] Y. K. Heng,[1,53,58] C. Herold,[55] G. Y. Hou,[1,58] Y. R. Hou,[58] Z. L. Hou,[1] H. M. Hu,[1,58] J. F. Hu,[51,i] T. Hu,[1,53,58] Y. Hu,[1] G. S. Huang,[66,53] K. X. Huang,[54] L. Q. Huang,[28,58] X. T. Huang,[45] Y. P. Huang,[1] Z. Huang,[42,g] T. Hussain,[68] N. Hüsken,[25,31] W. Imoehl,[25] M. Irshad,[66,53] J. Jackson,[25] S. Jaeger,[4] S. Janchiv,[29] E. Jang,[50] J. H. Jeong,[50] Q. Ji,[1] Q. P. Ji,[18] X. B. Ji,[1,58] X. L. Ji,[1,53] Y. Y. Ji,[45] Z. K. Jia,[66,53] H. B. Jiang,[45] S. S. Jiang,[35] X. S. Jiang,[1,53,58] Y. Jiang,[58] J. B. Jiao,[45] Z. Jiao,[21] S. Jin,[38] Y. Jin,[61] M. Q. Jing,[1,58] T. Johansson,[70] N. Kalantar-Nayestanaki,[59] X. S. Kang,[36] R. Kappert,[59] M. Kavatsyuk,[59] B. C. Ke,[75] I. K. Keshk,[4] A. Khoukaz,[63] R. Kiuchi,[1] R. Kliemt,[12] L. Koch,[33] O. B. Kolcu,[57a] B. Kopf,[4] M. Kuemmel,[4] M. Kuessner,[4] A. Kupsc,[40,70] W. Kühn,[33] J. J. Lane,[62] J. S. Lange,[33] P. Larin,[17] A. Lavania,[24] L. Lavezzi,[69a,69c] Z. H. Lei,[66,53] H. Leithoff,[31] M. Lellmann,[31] T. Lenz,[31] C. Li,[39] C. Li,[43] C. H. Li,[35] Cheng Li,[66,53] D. M. Li,[75] F. Li,[1,53] G. Li,[1] H. Li,[47] H. Li,[66,53] H. B. Li,[1,58] H. J. Li,[18] H. N. Li,[51,i] J. Q. Li,[4] J. S. Li,[54] J. W. Li,[45] Ke Li,[1] L. J. Li,[1] L. K. Li,[1] Lei Li,[3] M. H. Li,[39] P. R. Li,[34,j,k] S. X. Li,[10] S. Y. Li,[56] T. Li,[45] W. D. Li,[1,58] W. G. Li,[1] X. H. Li,[66,53] X. L. Li,[45] Xiaoyu Li,[1,58] Y. G. Li,[42,g] Z. X. Li,[14] H. Liang,[1,58] H. Liang,[30] H. Liang,[66,53] Y. F. Liang,[49] Y. T. Liang,[28,58] G. R. Liao,[13] L. Z. Liao,[45] J. Libby,[24] A. Limphirat,[55] C. X. Lin,[54] D. X. Lin,[28,58] T. Lin,[1] B. J. Liu,[1] C. X. Liu,[1] D. Liu,[17,66] F. H. Liu,[48] Fang Liu,[1] Feng Liu,[6] G. M. Liu,[51,i] H. Liu,[34,j,k] H. B. Liu,[14] H. M. Liu,[1,58] Huanhuan Liu,[1] Huihui Liu,[19] J. B. Liu,[66,53] J. L. Liu,[67] J. Y. Liu,[1,58] K. Liu,[1] K. Y. Liu,[36] Ke Liu,[20] L. Liu,[66,53] Lu Liu,[39] M. H. Liu,[10,f] P. L. Liu,[1] Q. Liu,[58] S. B. Liu,[66,53] T. Liu,[10,f] W. K. Liu,[39] W. M. Liu,[66,53] X. Liu,[34,j,k] Y. Liu,[34,j,k] Y. B. Liu,[39] Z. A. Liu,[1,53,58] Z. Q. Liu,[45] X. C. Lou,[1,53,58] F. X. Lu,[54] H. J. Lu,[21] J. G. Lu,[1,53] X. L. Lu,[1] Y. Lu,[7] Y. P. Lu,[1,53] Z. H. Lu,[1] C. L. Luo,[37] M. X. Luo,[74] T. Luo,[10,f] X. L. Luo,[1,53] X. R. Lyu,[58] Y. F. Lyu,[39] F. C. Ma,[36] H. L. Ma,[1] L. L. Ma,[45] M. M. Ma,[1,58] Q. M. Ma,[1] R. Q. Ma,[1,58] R. T. Ma,[58] X. Y. Ma,[1,53] Y. Ma,[42,g] F. E. Maas,[17] M. Maggiora,[69a,69c] S. Maldaner,[4] S. Malde,[64] Q. A. Malik,[68] A. Mangoni,[26b] Y. J. Mao,[42,g] Z. P. Mao,[1] S. Marcello,[69a,69c] Z. X. Meng,[61] J. Messchendorp,[12,59] G. Mezzadri,[27a] H. Miao,[1] T. J. Min,[38] R. E. Mitchell,[25] X. H. Mo,[1,53,58] N. Yu. Muchnoi,[11,b] Y. Nefedov,[32] F. Nerling,[17,d] I. B. Nikolaev,[11,b] Z. Ning,[1,53] S. Nisar,[9,l] Y. Niu,[45] S. L. Olsen,[58] Q. Ouyang,[1,53,58] S. Pacetti,[26b,26c] X. Pan,[10,f] Y. Pan,[52] A. Pathak,[30] M. Pelizaeus,[4] H. P. Peng,[66,53] K. Peters,[12,d] J. L. Ping,[37] R. G. Ping,[1,58] S. Plura,[31] S. Pogodin,[32] V. Prasad,[66,53] F. Z. Qi,[1] H. Qi,[66,53] H. R. Qi,[56] M. Qi,[38] T. Y. Qi,[10,f] S. Qian,[1,53] W. B. Qian,[58] Z. Qian,[54] C. F. Qiao,[58] J. J. Qin,[67] L. Q. Qin,[13] X. P. Qin,[10,f] X. S. Qin,[45] Z. H. Qin,[1,53] J. F. Qiu,[1] S. Q. Qu,[56] K. H. Rashid,[68] C. F. Redmer,[31] K. J. Ren,[35] A. Rivetti,[69c] V. Rodin,[59] M. Rolo,[69c] G. Rong,[1,58] Ch. Rosner,[17] S. N. Ruan,[39] H. S. Sang,[66] A. Sarantsev,[32,c] Y. Schelhaas,[31] C. Schnier,[4] K. Schoenning,[70] M. Scodeggio,[27a,27b] K. Y. Shan,[10,f] W. Shan,[22] X. Y. Shan,[66,53] J. F. Shangguan,[50] L. G. Shao,[1,58] M. Shao,[66,53] C. P. Shen,[10,f] H. F. Shen,[1,58] X. Y. Shen,[1,58] B. A. Shi,[58] H. C. Shi,[66,53] J. Y. Shi,[1] Q. Q. Shi,[50] R. S. Shi,[1,58] X. Shi,[1,53] X. D. Shi,[66,53] J. J. Song,[18] W. M. Song,[30,1] Y. X. Song,[42,g] S. Sosio,[69a,69c] S. Spataro,[69a,69c] F. Stieler,[31] K. X. Su,[71] P. P. Su,[50] Y. J. Su,[58] G. X. Sun,[1] H. Sun,[58] H. K. Sun,[1] J. F. Sun,[18] L. Sun,[71] S. S. Sun,[1,58] T. Sun,[1,58] W. Y. Sun,[30] X. Sun,[23,h] Y. J. Sun,[66,53] Y. Z. Sun,[1] Z. T. Sun,[45] Y. H. Tan,[71] Y. X. Tan,[66,53] C. J. Tang,[49] G. Y. Tang,[1] J. Tang,[54] L. Y. Tao,[67] Q. T. Tao,[23,h] M. Tat,[64] J. X. Teng,[66,53] V. Thoren,[70] W. H. Tian,[47] Y. Tian,[28,58] I. Uman,[57b] B. Wang,[1] B. L. Wang,[58] C. W. Wang,[38] D. Y. Wang,[42,g] F. Wang,[67] H. J. Wang,[34,j,k] H. P. Wang,[1,58] K. Wang,[1,53] L. L. Wang,[1] M. Wang,[45] M. Z. Wang,[42,g] Meng Wang,[1,58] S. Wang,[13] S. Wang,[10,f] T. Wang,[10,f] T. J. Wang,[39] W. Wang,[54] W. H. Wang,[71] W. P. Wang,[66,53] X. Wang,[42,g] X. F. Wang,[34,j,k] X. L. Wang,[10,f] Y. Wang,[56] Y. D. Wang,[41] Y. F. Wang,[1,53,58] Y. H. Wang,[43] Y. Q. Wang,[1] Yaqian Wang,[16,1] Z. Wang,[1,53] Z. Y. Wang,[1,58] Ziyi Wang,[58] D. H. Wei,[13] F. Weidner,[63] S. P. Wen,[1] D. J. White,[62] U. Wiedner,[4] G. Wilkinson,[64] M. Wolke,[70] L. Wollenberg,[4] J. F. Wu,[1,58] L. H. Wu,[1] L. J. Wu,[1,58] X. Wu,[10,f] X. H. Wu,[30] Y. Wu,[66] Y. J. Wu,[28] Z. Wu,[1,53] L. Xia,[66,53] T. Xiang,[42,g] D. Xiao,[34,j,k] G. Y. Xiao,[38] H. Xiao,[10,f] S. Y. Xiao,[1]

Y. L. Xiao,[10,f] Z. J. Xiao,[37] C. Xie,[38] X. H. Xie,[42,g] Y. Xie,[45] Y. G. Xie,[1,53] Y. H. Xie,[6] Z. P. Xie,[66,53] T. Y. Xing,[1,58] C. F. Xu,[1] C. J. Xu,[54] G. F. Xu,[1] H. Y. Xu,[61] Q. J. Xu,[15] X. P. Xu,[50] Y. C. Xu,[58] Z. P. Xu,[38] F. Yan,[10,f] L. Yan,[10,f] W. B. Yan,[66,53] W. C. Yan,[75] H. J. Yang,[46,e] H. L. Yang,[30] H. X. Yang,[1] L. Yang,[47] S. L. Yang,[58] Tao Yang,[1] Y. F. Yang,[39] Y. X. Yang,[1,58] Yifan Yang,[1,58] M. Ye,[1,53] M. H. Ye,[8] J. H. Yin,[1] Z. Y. You,[54] B. X. Yu,[1,53,58] C. X. Yu,[39] G. Yu,[1,58] T. Yu,[67] X. D. Yu,[42,g] C. Z. Yuan,[1,58] L. Yuan,[2] S. C. Yuan,[1] X. Q. Yuan,[1] Y. Yuan,[1,58] Z. Y. Yuan,[54] C. X. Yue,[35] A. A. Zafar,[68] F. R. Zeng,[45] X. Zeng,[6] Y. Zeng,[23,h] Y. H. Zhan,[54] A. Q. Zhang,[1] B. L. Zhang,[1] B. X. Zhang,[1] D. H. Zhang,[39] G. Y. Zhang,[18] H. Zhang,[66] H. H. Zhang,[54] H. H. Zhang,[30] H. Y. Zhang,[1,53] J. L. Zhang,[72] J. Q. Zhang,[37] J. W. Zhang,[1,53,58] J. X. Zhang,[34,j,k] J. Y. Zhang,[1] J. Z. Zhang,[1,58] Jianyu Zhang,[1,58] Jiawei Zhang,[1,58] L. M. Zhang,[56] L. Q. Zhang,[54] Lei Zhang,[38] P. Zhang,[1] Q. Y. Zhang,[35,75] Shuihan Zhang,[1,58] Shulei Zhang,[23,h] X. D. Zhang,[41] X. M. Zhang,[1] X. Y. Zhang,[50] X. Y. Zhang,[45] Y. Zhang,[64] Y. T. Zhang,[75] Y. H. Zhang,[1,53] Yan Zhang,[66,53] Yao Zhang,[1] Z. H. Zhang,[1] Z. Y. Zhang,[71] Z. Y. Zhang,[39] G. Zhao,[1] J. Zhao,[35] J. Y. Zhao,[1,58] J. Z. Zhao,[1,53] Lei Zhao,[66,53] Ling Zhao,[1] M. G. Zhao,[39] Q. Zhao,[1] S. J. Zhao,[75] Y. B. Zhao,[1,53] Y. X. Zhao,[28,58] Z. G. Zhao,[66,53] A. Zhemchugov,[32,a] B. Zheng,[67] J. P. Zheng,[1,53] Y. H. Zheng,[58] B. Zhong,[37] C. Zhong,[67] X. Zhong,[54] H. Zhou,[45] L. P. Zhou,[1,58] X. Zhou,[71] X. K. Zhou,[58] X. R. Zhou,[66,53] X. Y. Zhou,[35] Y. Z. Zhou,[10,f] J. Zhu,[39] K. Zhu,[1] K. J. Zhu,[1,53,58] L. X. Zhu,[58] S. H. Zhu,[65] S. Q. Zhu,[38] T. J. Zhu,[72] W. J. Zhu,[10,f] Y. C. Zhu,[66,53] Z. A. Zhu,[1,58] B. S. Zou,[1] and J. H. Zou[1]

(BESIII Collaboration)

[1]*Institute of High Energy Physics, Beijing 100049, People's Republic of China*
[2]*Beihang University, Beijing 100191, People's Republic of China*
[3]*Beijing Institute of Petrochemical Technology, Beijing 102617, People's Republic of China*
[4]*Bochum Ruhr-University, D-44780 Bochum, Germany*
[5]*Carnegie Mellon University, Pittsburgh, Pennsylvania 15213, USA*
[6]*Central China Normal University, Wuhan 430079, People's Republic of China*
[7]*Central South University, Changsha 410083, People's Republic of China*
[8]*China Center of Advanced Science and Technology, Beijing 100190, People's Republic of China*
[9]*COMSATS University Islamabad, Lahore Campus, Defence Road, Off Raiwind Road, 54000 Lahore, Pakistan*
[10]*Fudan University, Shanghai 200433, People's Republic of China*
[11]*G.I. Budker Institute of Nuclear Physics SB RAS (BINP), Novosibirsk 630090, Russia*
[12]*GSI Helmholtzcentre for Heavy Ion Research GmbH, D-64291 Darmstadt, Germany*
[13]*Guangxi Normal University, Guilin 541004, People's Republic of China*
[14]*Guangxi University, Nanning 530004, People's Republic of China*
[15]*Hangzhou Normal University, Hangzhou 310036, People's Republic of China*
[16]*Hebei University, Baoding 071002, People's Republic of China*
[17]*Helmholtz Institute Mainz, Staudinger Weg 18, D-55099 Mainz, Germany*
[18]*Henan Normal University, Xinxiang 453007, People's Republic of China*
[19]*Henan University of Science and Technology, Luoyang 471003, People's Republic of China*
[20]*Henan University of Technology, Zhengzhou 450001, People's Republic of China*
[21]*Huangshan College, Huangshan 245000, People's Republic of China*
[22]*Hunan Normal University, Changsha 410081, People's Republic of China*
[23]*Hunan University, Changsha 410082, People's Republic of China*
[24]*Indian Institute of Technology Madras, Chennai 600036, India*
[25]*Indiana University, Bloomington, Indiana 47405, USA*
[26a]*INFN Laboratori Nazionali di Frascati, I-00044, Frascati, Italy*
[26b]*INFN Sezione di Perugia, I-06100, Perugia, Italy*
[26c]*University of Perugia, I-06100, Perugia, Italy*
[27a]*INFN Sezione di Ferrara, I-44122, Ferrara, Italy;*
[27b]*University of Ferrara, I-44122, Ferrara, Italy*
[28]*Institute of Modern Physics, Lanzhou 730000, People's Republic of China*
[29]*Institute of Physics and Technology, Peace Avenue 54B, Ulaanbaatar 13330, Mongolia*
[30]*Jilin University, Changchun 130012, People's Republic of China*
[31]*Johannes Gutenberg University of Mainz, Johann-Joachim-Becher-Weg 45, D-55099 Mainz, Germany*
[32]*Joint Institute for Nuclear Research, 141980 Dubna, Moscow region, Russia*
[33]*Justus-Liebig-Universitaet Giessen, II. Physikalisches Institut, Heinrich-Buff-Ring 16, D-35392 Giessen, Germany*
[34]*Lanzhou University, Lanzhou 730000, People's Republic of China*
[35]*Liaoning Normal University, Dalian 116029, People's Republic of China*

[36]Liaoning University, Shenyang 110036, People's Republic of China
[37]Nanjing Normal University, Nanjing 210023, People's Republic of China
[38]Nanjing University, Nanjing 210093, People's Republic of China
[39]Nankai University, Tianjin 300071, People's Republic of China
[40]National Centre for Nuclear Research, Warsaw 02-093, Poland
[41]North China Electric Power University, Beijing 102206, People's Republic of China
[42]Peking University, Beijing 100871, People's Republic of China
[43]Qufu Normal University, Qufu 273165, People's Republic of China
[44]Shandong Normal University, Jinan 250014, People's Republic of China
[45]Shandong University, Jinan 250100, People's Republic of China
[46]Shanghai Jiao Tong University, Shanghai 200240, People's Republic of China
[47]Shanxi Normal University, Linfen 041004, People's Republic of China
[48]Shanxi University, Taiyuan 030006, People's Republic of China
[49]Sichuan University, Chengdu 610064, People's Republic of China
[50]Soochow University, Suzhou 215006, People's Republic of China
[51]South China Normal University, Guangzhou 510006, People's Republic of China
[52]Southeast University, Nanjing 211100, People's Republic of China
[53]State Key Laboratory of Particle Detection and Electronics, Beijing 100049, Hefei 230026, People's Republic of China
[54]Sun Yat-Sen University, Guangzhou 510275, People's Republic of China
[55]Suranaree University of Technology, University Avenue 111, Nakhon Ratchasima 30000, Thailand
[56]Tsinghua University, Beijing 100084, People's Republic of China
[57a]Turkish Accelerator Center Particle Factory Group, Istinye University, 34010, Istanbul, Turkey
[57b]Near East University, Nicosia, North Cyprus, Mersin 10, Turkey
[58]University of Chinese Academy of Sciences, Beijing 100049, People's Republic of China
[59]University of Groningen, NL-9747 AA Groningen, The Netherlands
[60]University of Hawaii, Honolulu, Hawaii 96822, USA
[61]University of Jinan, Jinan 250022, People's Republic of China
[62]University of Manchester, Oxford Road, Manchester, M13 9PL, United Kingdom
[63]University of Muenster, Wilhelm-Klemm-Strasse 9, 48149 Muenster, Germany
[64]University of Oxford, Keble Road, Oxford OX13RH, United Kingdom
[65]University of Science and Technology Liaoning, Anshan 114051, People's Republic of China
[66]University of Science and Technology of China, Hefei 230026, People's Republic of China
[67]University of South China, Hengyang 421001, People's Republic of China
[68]University of the Punjab, Lahore-54590, Pakistan
[69a]University of Turin, I-10125, Turin, Italy
[69b]University of Eastern Piedmont, I-15121, Alessandria, Italy
[69c]INFN, I-10125, Turin, Italy
[70]Uppsala University, Box 516, SE-75120 Uppsala, Sweden
[71]Wuhan University, Wuhan 430072, People's Republic of China
[72]Xinyang Normal University, Xinyang 464000, People's Republic of China
[73]Yunnan University, Kunming 650500, People's Republic of China
[74]Zhejiang University, Hangzhou 310027, People's Republic of China
[75]Zhengzhou University, Zhengzhou 450001, People's Republic of China

[a]Also at the Moscow Institute of Physics and Technology, Moscow 141700, Russia.
[b]Also at the Novosibirsk State University, Novosibirsk, 630090, Russia.
[c]Also at the NRC "Kurchatov Institute", PNPI, 188300, Gatchina, Russia.
[d]Also at Goethe University Frankfurt, 60323 Frankfurt am Main, Germany.
[e]Also at Key Laboratory for Particle Physics, Astrophysics and Cosmology, Ministry of Education; Shanghai Key Laboratory for Particle Physics and Cosmology; Institute of Nuclear and Particle Physics, Shanghai 200240, People's Republic of China.
[f]Also at Key Laboratory of Nuclear Physics and Ion-beam Application (MOE) and Institute of Modern Physics, Fudan University, Shanghai 200443, People's Republic of China.
[g]Also at State Key Laboratory of Nuclear Physics and Technology, Peking University, Beijing 100871, People's Republic of China.
[h]Also at School of Physics and Electronics, Hunan University, Changsha 410082, China.
[i]Also at Guangdong Provincial Key Laboratory of Nuclear Science, Institute of Quantum Matter, South China Normal University, Guangzhou 510006, China.
[j]Also at Frontiers Science Center for Rare Isotopes, Lanzhou University, Lanzhou 730000, People's Republic of China.
[k]Also at Lanzhou Center for Theoretical Physics, Lanzhou University, Lanzhou 730000, People's Republic of China.
[l]Also at the Department of Mathematical Sciences, IBA, Karachi, Pakistan.

(Received 5 January 2023; accepted 10 February 2023; published 27 February 2023)

Based on 7.33 fb^{-1} of e^+e^- collision data taken at center-of-mass energies between 4.128 and 4.226 GeV with the BESIII detector, we measure the branching fraction of $D_s^{*+} \to D_s^+\pi^0$ relative to that of $D_s^{*+} \to D_s^+\gamma$ to be $(6.16 \pm 0.43 \pm 0.18)\%$. The first uncertainty is statistical and the second one is systematic. By using the world average value of the branching fraction of $D_s^{*+} \to D_s^+e^+e^-$, we determine the branching fractions of $D_s^{*+} \to D_s^+\gamma$ and $D_s^{*+} \to D_s^+\pi^0$ to be $(93.57 \pm 0.38 \pm 0.22)\%$ and $(5.76 \pm 0.38 \pm 0.16)\%$, respectively.

DOI: 10.1103/PhysRevD.107.032011

I. INTRODUCTION

The excited strange charmed meson, D_s^{*+}, is formed from $c\bar{s}$ quark-antiquark pair. Throughout this paper, charge-conjugate states are always included. Due to the quark SU(2) flavor-breaking effects, the D_s^{*+} decays are dominated by the radiative process $D_s^{*+} \to D_s^+\gamma$ and the isospin-violating hadronic process $D_s^{*+} \to D_s^+\pi^0$. Measurements of the branching fractions (BFs) of the D_s^{*+} decays are important to explore quantum chromodynamics (QCD) [1] describing the strong interaction in the Standard Model of particle physics. The decay widths of $D_s^{*+} \to D_s^+\gamma$ and/or $D_s^{*+} \to D_s^+\pi^0$ have been theoretically predicted based on effective phenomenological models, e.g. the chiral perturbation theory (χPT) [2–5], the light-front quark model (LFQM) [6], the relativistic quark model (RQM) [7], the QCD sum rules (QCDSR) [8,9], the Nambu-Jona-Lasinio model (NJLM) [10], the lattice QCD (LQCD) [11], the nonrelativistic quark model (NRQM) [12,13], and the covariant model (CM) [14]. The BF of $D_s^{*+} \to D_s^+\pi^0$ relative to that of $D_s^{*+} \to D_s^+\gamma$ has been measured by using e^+e^- collision data accumulated at the $\Upsilon(3S)$ and $\Upsilon(4S)$ by the CLEO [15] and *BABAR* [16] experiments. The precision of the world average of the BF of $D_s^{*+} \to D_s^+\gamma$ is about 0.7% [17]. Precision measurements of these BFs help to constrain the parameters of the low-energy effective models. In addition, the BFs are important inputs in the precise determination of the D_s^+ decay constant $f_{D_s^+}$ and the $c \to s$ Cabibbo-Kobayashi-Maskawa matrix element $|V_{cs}|$ via the $e^+e^- \to D_s^{*\pm}D_s^{\mp}$ processes.

In this paper, we report an improved measurement of the BF of $D_s^{*+} \to D_s^+\pi^0$ relative to $D_s^{*+} \to D_s^+\gamma$ and then determine the BFs of $D_s^{*+} \to D_s^+\gamma$ and $D_s^{*+} \to D_s^+\pi^0$. This analysis is carried out by using 7.33 fb^{-1} of e^+e^- collision data taken at center-of-mass energies $E_{\rm cm}$ between 4.128 and 4.226 GeV with the BESIII detector.

II. BESIII DETECTOR AND MONTE CARLO

The BESIII detector [18] records symmetric e^+e^- collisions provided by the BEPCII storage ring [19] in the center-of-mass energy range from 2.0 to 4.95 GeV, with a peak luminosity of 1×10^{33} cm^{-2} s^{-1} achieved at $\sqrt{s} = 3.773$ GeV. BESIII has collected large data samples in this energy region [20]. BESIII is a cylindrical spectrometer with a geometrical acceptance of 93% over the 4π solid angle. It consists of a helium-based multilayer drift chamber (MDC), a plastic scintillator time-of-flight system (TOF), and a CsI(Tl) electromagnetic calorimeter (EMC), which are all enclosed in a superconducting solenoidal magnet providing a 1.0 T magnetic field. The solenoid is supported by an octagonal flux-return yoke with resistive plate counter muon identifier modules interleaved with steel [21]. The charged particle momentum resolution is 0.5% at 1 GeV/c, and the specific energy loss (dE/dx) resolution is 6% for the electrons from Bhabha scattering. The EMC measures photon energies with a resolution of 2.5% (5%) at 1 GeV in the barrel (end-cap) region. The time resolution in the TOF barrel region is 68 ps. The end-cap TOF system was upgraded in 2015 using multigap resistive plate chamber technology, providing a time resolution of 60 ps [22]. Approximately 83% of the data used here was collected after this upgrade; luminosities [23] at each energy, with a total uncertainty of about 1%, are given in Table I.

Simulated data samples are produced with a GEANT4-based [24] Monte Carlo (MC) toolkit including the geometric description of the BESIII detector and the detector

TABLE I. The integrated luminosity and $M_{\rm BC}$ requirement for each energy ($E_{\rm cm}$) point.

$E_{\rm cm}$ (GeV)	Luminosity (pb^{-1})	$M_{\rm BC}$ (GeV/c^2)
4.128	401.5	[2.010, 2.061]
4.157	408.7	[2.010, 2.070]
4.178	3189.0	[2.010, 2.073]
4.189	569.8	[2.010, 2.076]
4.199	526.0	[2.010, 2.079]
4.209	571.7	[2.010, 2.082]
4.219	568.7	[2.010, 2.085]
4.226	1091.7	[2.010, 2.088]

response. The simulation includes the beam energy spread and initial state radiation (ISR) in the e^+e^- annihilations with the generator KKMC [25]. In the MC simulation, the production of open-charm processes directly produced via e^+e^- annihilations are modeled with the generator CONEXC [26]. The ISR production of vector charmonium(-like) states and the continuum processes are incorporated in KKMC [25]. All particle decays are modeled with EVTGEN [27] using BFs either taken from the Particle Data Group [17], when available, or otherwise estimated with LUNDCHARM [28]. Final state radiation (FSR) from charged final state particles is incorporated using PHOTOS [29].

The input cross section line shape of $e^+e^- \to D_s^{*\pm}D_s^{\mp}$ is based on the results in Ref. [30]. In this analysis, the inclusive MC sample, which is generated at various energy points and has an integrated luminosity equivalent to 40 times the sample size in data, is used to determine detection efficiencies and to estimate background contributions.

III. EVENT SELECTION

At the center-of-mass energies between 4.128 and 4.226 GeV, $D_s^{*+}D_s^-$ pairs are produced copiously by e^+e^- collisions. The D_s^{*+} mesons decay predominantly via $D_s^{*+} \to D_s^+\gamma$ and $D_s^{*+} \to D_s^+\pi^0$. Candidate events are selected by reconstructing D_s^+ and D_s^- mesons via hadronic decay modes. To obtain better momentum resolution and lower background contamination, we use three pairs of decay modes, labeled as modes I, II, and III, respectively: $D_s^+ \to K^+K^-\pi^+$ versus $D_s^- \to K^+K^-\pi^-$, $D_s^+ \to K^+K^-\pi^+$ versus $D_s^- \to K_S^0K^-$, and $D_s^+ \to K_S^0K^+$ versus $D_s^- \to K_S^0K^-$. In order to improve detection efficiencies no transition photon or π^0 from the D_s^{*+} decay is required.

Charged tracks detected in the MDC are required to be within a polar angle (θ) range of $|\cos\theta| < 0.93$, where θ is defined with respect to the z axis, which is the symmetry axis of the MDC. For charged tracks not originating from K_S^0 decays, the distance of closest approach to the interaction point (IP) must be less than 10 cm along the z axis, $|V_z|$ and less than 1 cm in the transverse plane $|V_{xy}|$. No additional charged track passing the $\cos\theta$ and IP cuts is allowed for selected candidates. Particle identification for charged tracks combines measurements of the dE/dx in the MDC and the flight time in the TOF to form likelihoods for charged pion and kaon hypotheses, $\mathcal{L}(\pi)$ and $\mathcal{L}(K)$. Pion candidates are required to satisfy $\mathcal{L}(\pi) > \mathcal{L}(K)$ and $\mathcal{L}(\pi) > 0$, and kaon candidates are required to satisfy $\mathcal{L}(K) > \mathcal{L}(\pi)$ and $\mathcal{L}(K) > 0$.

The K_S^0 candidates are reconstructed via the decay $K_S^0 \to \pi^+\pi^-$. The two charged pions are required to satisfy $|V_z| < 20$ cm and $|\cos\theta| < 0.93$ but no particle identification is applied. The $\pi^+\pi^-$ invariant mass is required to be within the interval $(0.487, 0.511)$ GeV/c^2. A vertex fit is performed, constraining the two tracks to originate from a common vertex, and the decay length of any K_S^0 candidate is required to be greater than twice its resolution.

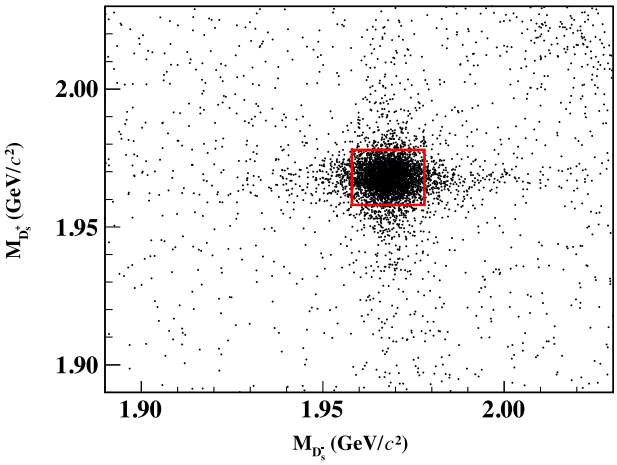

FIG. 1. The distribution of $M_{D_s^-}$ versus $M_{D_s^+}$ summing over modes I, II, and III in data. The red rectangle denotes the signal region.

To suppress non-$D_s^{\pm}D_s^{*\mp}$ events, the beam-constrained mass of the D_s^- candidate,

$$M_{\rm BC} \equiv \sqrt{E_{\rm beam}^2 - |\vec{p}_{\rm tag}|^2}, \quad (1)$$

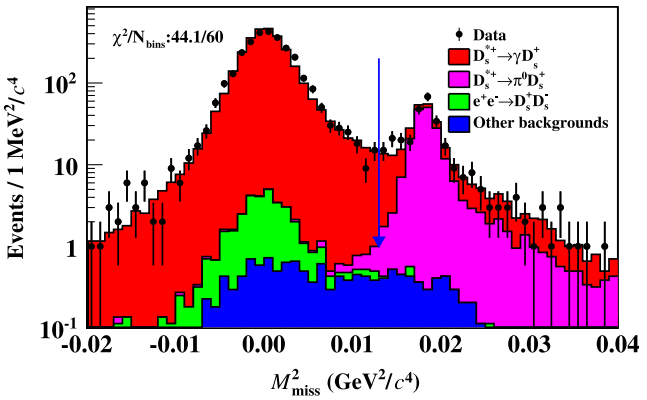

FIG. 2. The $M^2_{\rm miss}$ distribution of the accepted candidates, summing over modes I, II, and III. The points with error bars are data, the red histogram is the total simulated MC sample, obtained by adding the scaled signal component $D_s^{*+} \to D_s^+\gamma$ to the magenta histogram. The magenta histogram is composed of the signal component $D_s^{*+} \to D_s^+\pi^0$, the exclusive decay $e^+e^- \to D_s^+D_s^-$ (filled green histogram), and the inclusive background (filled blue histogram). The filled green and blue histograms are from $e^+e^- \to D_s^+D_s^-$ and other background events, respectively, estimated from the inclusive MC sample. The histograms shown here are stacked histograms, plotted with the explicit component labeled in the legend added to the components already summed in the histograms below. The blue vertical arrow shows the dividing line for $D_s^{*+} \to D_s^+\gamma$ and $D_s^{*+} \to D_s^+\pi^0$ candidates. The χ^2 test [31] result for comparison of the data and weighted MC histograms is also shown, with $N_{\rm bins}$ as the number of histogram bins.

TABLE II. The quantities used for f_γ measurements and the obtained results. The average result is weighted over modes I, II, and III by their inverse statistical uncertainties squared. The uncertainties are statistical only.

Mode	$N_\gamma^{\rm obs}$	$N_{\pi^0}^{\rm obs}$	$N_\gamma^{\rm bkg}$	$N_{\pi^0}^{\rm bkg}$	$\epsilon_{\gamma\gamma}(\%)$	$\epsilon_{\gamma\pi^0}(\%)$	$\epsilon_{\pi^0\gamma}(\%)$	$\epsilon_{\pi^0\pi^0}(\%)$	$f_\gamma(\%)$
I	2293.0 ± 47.9	239.0 ± 15.5	31.0 ± 0.9	5.0 ± 0.4	14.16 ± 0.04	0.42 ± 0.01	0.22 ± 0.02	15.08 ± 0.17	93.52 ± 0.49
II	1044.0 ± 32.3	83.0 ± 9.1	12.0 ± 0.5	1.0 ± 0.2	15.97 ± 0.07	0.46 ± 0.01	0.16 ± 0.03	16.38 ± 0.29	95.32 ± 0.63
III	119.0 ± 10.9	11.0 ± 3.3	1.0 ± 0.2	0.0 ± 0.0	17.27 ± 0.23	0.52 ± 0.05	0.00 ± 0.00	18.08 ± 0.96	94.31 ± 2.04
Average									94.20 ± 0.38

is required to be within the intervals shown in Table I. Here, $E_{\rm beam}$ is the beam energy, and $\vec{p}_{\rm tag}$ is the three-momenta of the reconstructed D_s^- candidate in the e^+e^- center-of-mass frame. In each event, we only keep one candidate per tag mode per charge, selecting the one with the D_s^- recoil mass

$$M_{\rm rec} \equiv \sqrt{(E_{\rm cm} - \sqrt{|\vec{p}_{\rm tag}|^2 + m_{D_s}^2})^2 - |\vec{p}_{\rm tag}|^2}, \quad (2)$$

closest to the nominal D_s^{*+} mass [17]. The D_s^+ candidate is selected in the presence of the tag D_s^-. If there are multiple D_s^+ combinations in an event, then the one giving the minimum $|M_{D_s^+} + M_{D_s^-} - 2m_{D_s}|$ is retained for further analysis. Here $M_{D_s^\pm}$ is the invariant mass of the $D_s^\pm$ candidate, and m_{D_s} is the nominal D_s mass [17]. Figure 1 shows the distribution of $M_{D_s^-}$ versus $M_{D_s^+}$ of the accepted candidates in data. To suppress background, the invariant masses of $K^+K^-\pi^\pm$ and $K_S^0K^\pm$ combinations are required to be within the interval $M_{D_s^\pm} \in (1.958, 1.978)$ GeV/c^2.

To improve momentum resolution, a two-constraint kinematic fit, in which the invariant mass of the $K^+K^-\pi^\pm$ or $K_S^0K^\pm$ combination is constrained to the known D_s mass [17] is performed. The momenta updated by the kinematic fit are kept for further analysis.

To separate the $D_s^{*+} \to D_s^+\gamma$ and $D_s^{*+} \to D_s^+\pi^0$ candidates, we define the missing mass squared of the reconstructed $D_s^+D_s^-$ combination as

$$M_{\rm miss}^2 \equiv (E_{\rm cm} - E_{D_s^+} - E_{D_s^-})^2 - |-\vec{p}_{D_s^+} - \vec{p}_{D_s^-}|^2, \quad (3)$$

where $E_{D_s^\pm}$ and $\vec{p}_{D_s^\pm}$ are the energy and momentum of $D_s^\pm$ in the e^+e^- center-of-mass system, respectively. The resultant $M_{\rm miss}^2$ distribution of the accepted $D_s^+D_s^-$ candidate combinations is shown in Fig. 2, where the peak near zero and the right-side peak correspond to $D_s^{*+} \to D_s^+\gamma$ and $D_s^{*+} \to D_s^+\pi^0$ candidates, respectively.

IV. BRANCHING FRACTIONS

Following Ref. [32], the BF of $D_s^{*+} \to D_s^+\gamma$ relative to the sum of $D_s^{*+} \to D_s^+\gamma$ and $D_s^{*+} \to D_s^+\pi^0$ is determined by

$$f_\gamma = \frac{\mathcal{B}_{D_s^{*+}\to D_s^+\gamma}}{\mathcal{B}_{D_s^{*+}\to D_s^+\gamma} + \mathcal{B}_{D_s^{*+}\to D_s^+\pi^0}} = \frac{N_\gamma^{\rm prod}}{N_\gamma^{\rm prod} + N_{\pi^0}^{\rm prod}}, \quad (4)$$

where $N_\gamma^{\rm prod}$ and $N_{\pi^0}^{\rm prod}$ are the numbers of produced $D_s^{*+} \to D_s^+\gamma$ and $D_s^{*+} \to D_s^+\pi^0$ events, respectively. This ratio captures the binomial nature of the separation of the low-background signal into the two decays under study.

As shown in Fig. 2, the individual signal regions of $M_{\rm miss}^2$ are defined as $[-0.020, 0.013]$ and $[0.013, 0.040]$ GeV$^2/c^4$ for $D_s^{*+} \to D_s^+\gamma$ and $D_s^{*+} \to D_s^+\pi^0$, respectively. The dividing line accepts about 99.0% of the $D^{*+} \to D_s^+\gamma$ signal and about 98.5% of the $D_s^{*+} \to D_s^+\pi^0$ signal. Due to the overlapping $M_{\rm miss}^2$ distributions, some $D_s^{*+} \to D_s^+\gamma$ events can be misidentified as $D_s^{*+} \to D_s^+\pi^0$ and vice versa. To account for this effect, the yields of $N_\gamma^{\rm prod}$ and $N_{\pi^0}^{\rm prod}$ are obtained by solving the following equation:

$$\begin{pmatrix} N_\gamma^{\rm obs} - N_\gamma^{\rm bkg} \\ N_{\pi^0}^{\rm obs} - N_{\pi^0}^{\rm bkg} \end{pmatrix} = \begin{pmatrix} \epsilon_{\gamma\gamma} & \epsilon_{\pi^0\gamma} \\ \epsilon_{\gamma\pi^0} & \epsilon_{\pi^0\pi^0} \end{pmatrix} \begin{pmatrix} N_\gamma^{\rm prod} \\ N_{\pi^0}^{\rm prod} \end{pmatrix}, \quad (5)$$

where $N_i^{\rm obs}$ is the number of selected events in data, $N_i^{\rm bkg}$ is the number of background events estimated from the inclusive MC sample, and ϵ_{ij} is the efficiency of the generated $D_s^{*+} \to D_s^+ + i$ events selected as $D_s^{*+} \to D_s^+ + j$, where i and j denote γ or π^0. To consider different detection efficiencies for ISR and FSR effects, the detection efficiencies at various energy points have been weighted by individual single tag D_s^+ yields in data. The background rates estimated from the inclusive MC sample for modes I, II, and III are all less than 1.5%.

Table II lists the quantities used for the f_γ measurements and the results obtained. Weighting the f_γ results for modes I, II, and III by their inverse

TABLE III. Relative systematic uncertainties in the determination of f_γ.

Source	Uncertainty (%)
$M_{\rm miss}^2$ resolution	0.07
MC statistics	0.12
Background	0.10
Sum	0.17

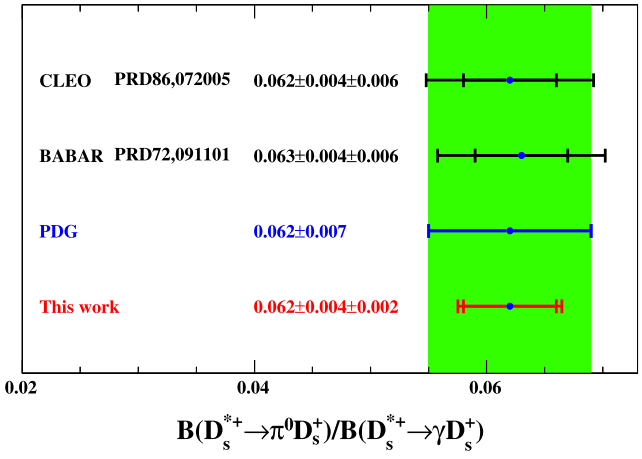

FIG. 3. Comparison of $\mathcal{B}_{D_s^{*+}\to D_s^+\pi^0}/\mathcal{B}_{D_s^{*+}\to D_s^+\gamma}$ measured by this work and previous experiments. The points with error bars are from different experiments. For each experiment, the shorter error bar denotes statistical only, while the longer error bar combines both statistical and systematic uncertainties. The green band corresponds to the $\pm 1\sigma$ limit of the world average.

statistical uncertainties squared, we obtain their average $f_\gamma = (94.20 \pm 0.38)\%$.

V. SYSTEMATIC UNCERTAINTIES

The systematic uncertainties in the BF measurements are discussed below. The systematic uncertainty due to $M^2_{\rm miss}$ resolution is examined in the following procedure. We perform a fit to $M^2_{\rm miss}$ distribution of data. To take into account the resolution difference between data and MC simulation, a signal MC shape smeared with a Gaussian function is used. From the fit, we obtain the parameters (means, widths) of the Gaussian resolution functions, which are $(1.0 \pm 0.1,\ 1.0 \pm 0.2)$, $(1.1 \pm 0.1,\ 1.0 \pm 0.2)$, and $(0.4 \pm 0.3, 1.7 \pm 0.4)$ MeV$^2/c^4$ for modes I, II, and III, respectively. The change of BF before and after smearing the Gaussian resolution function to the $M^2_{\rm miss}$ distribution of the signal MC events, 0.07%, is taken as the associated systematic uncertainty.

The systematic uncertainty caused by the statistical uncertainty of the MC efficiencies is estimated by varying each of the efficiency matrix elements by $\pm 1\sigma$. The largest change of the BF is taken as the systematic uncertainty.

The systematic uncertainty from background estimation is considered in two parts. The number of background events is calculated from the inclusive MC sample. The corresponding systematic uncertainty is estimated from the uncertainties of the cross sections used in generating this sample. The dominant background events are from open charm processes of $e^+e^- \to D_s^+D_s^-$ and $e^+e^- \to D_s^{*+}D_s^-$. The systematic uncertainty is estimated by varying the cross sections and BFs of the hadronic D_s^+ decays by $\pm 1\sigma$. This effect on the BF measurement is negligible. In addition, we have also varied the simulated background events by the ratio of the background events observed in the $D_s^+D_s^-$ sideband regions between data and the inclusive MC sample. The change of the BF, 0.10%, is taken as the corresponding systematic uncertainty. Other possible systematic uncertainty sources, such as the ISR simulation, the kinematic fit, the tracking and particle identification efficiencies between the two decay modes of D_s^{*+}, the $M_{\rm BC}$ requirement and the $M^2_{\rm miss}$ range, have also been investigated. All of them are negligible.

TABLE IV. Comparisons of the partial widths (Γ) and BFs (in brackets). The decay widths are in units of keV. The first two rows are from this work and the Particle Data Group, while the others are from various theoretical predictions. The superscript [a] denotes the value corresponding to $g = 0.52$, $\beta = 2.6$ GeV^{-1}, and $m_c = 1.6$ GeV; [b] denotes the values for a linear model; [c] denotes the value for $\kappa^q = 0.55$; and [d] denotes the values for (a) model.

	$\Gamma[\mathcal{B}]_{D_s^*\to D_s^+\gamma}$	$\Gamma[\mathcal{B}]_{D_s^*\to D_s^+\pi^0}$	$\mathcal{B}_{D_s^{*+}\to D_s^+\pi^0}/\mathcal{B}_{D_s^{*+}\to D_s^+\gamma}$
This work	…[$(93.57 \pm 0.38 \pm 0.22)\%$]	…[$(5.76 \pm 0.38 \pm 0.16)\%$]	$(6.16 \pm 0.43 \pm 0.18)\%$
PDG [17]	…[$(94.2 \pm 0.7)\%$]	…[$(5.9 \pm 0.7)\%$]	$(6.2 \pm 0.8)\%$
CM [14]	3.53 [$(92.7 \pm 0.7)\%$]	$0.277^{+0.028}_{-0.026}$ [$(7.3 \pm 0.7)\%$]	$(7.9 \pm 0.8)\%$
χPT [2][a]	4.5	…	…
χPT [3]	…	…	$8 \times 10^{-5}/\mathcal{B}(D^{*+} \to D^+\gamma)$
χPT [4]	0.32 ± 0.30	…	…
χPT [5]	…	$0.0081^{+0.0030}_{-0.0026}$	…
LFQM [6][b]	0.18 ± 0.01	…	…
RQM [7][c]	$0.321^{+0.009}_{-0.008}$	…	…
QCDSR [8]	0.25 ± 0.08	…	…
QCDSR [9]	0.59 ± 0.15	…	…
NJLM [10]	0.09	…	…
LQCD [11]	0.066 ± 0.026	…	…
NRQM [12]	0.21	…	…
NRQM [13][d]	0.40	…	…

All systematic uncertainties are summarized in Table III. Assuming the systematic uncertainties from different sources are independent, the total systematic uncertainty is obtained to be 0.17% by adding all the sources quadratically.

VI. SUMMARY

By analyzing 7.33 fb^{-1} of e^+e^- collision data taken at center-of-mass energies between 4.128 and 4.226 GeV, we measure the BF of $D_s^{*+} \to D_s^+\gamma$ relative to the sum of $D_s^{*+} \to D_s^+\gamma$ and $D_s^{*+} \to D_s^+\pi^0$ to be $f_\gamma = (94.20 \pm 0.38 \pm 0.16)\%$. This gives the BF of $D_s^{*+} \to D_s^+\pi^0$ relative to that of $D_s^{*+} \to D_s^+\gamma$ to be $\mathcal{B}_{D_s^{*+}\to D_s^+\pi^0}/\mathcal{B}_{D_s^{*+}\to D_s^+\gamma} = \frac{1}{f_\gamma} - 1 = (6.16 \pm 0.43 \pm 0.18)\%$. The D_s^{*+} is known to decay dominantly into three final states of $D_s^+\gamma$, $D_s^+\pi^0$ and $D_s^+e^+e^-$ [14]. Combining the world average of $\mathcal{B}_{D_s^{*+}\to D_s^+e^+e^-} = (0.67 \pm 0.16)\%$ [17], we obtain $\mathcal{B}_{D_s^{*+}\to D_s^+\gamma} = (93.57 \pm 0.38 \pm 0.22)\%$ and $\mathcal{B}_{D_s^{*+}\to D_s^+\pi^0} = (5.76 \pm 0.38 \pm 0.16)\%$, where the second errors include an additional uncertainty from the quoted $\mathcal{B}_{D_s^{*+}\to D_s^+e^+e^-}$.

Figure 3 shows the comparison of the measured BF of $\mathcal{B}_{D_s^{*+}\to D_s^+\pi^0}/\mathcal{B}_{D_s^{*+}\to D_s^+\gamma}$ with other experiments and the world-average value [17]. Our measurement is consistent with the previous ones but with better precision. Table IV shows comparisons of the BFs measured in this work with the world-average values and the decay widths or BFs predicted by various theories. Our results of $\mathcal{B}_{D_s^*\to D_s^+\gamma}$ and $\mathcal{B}_{D_s^*\to D_s^+\pi^0}$ are consistent with those predicted in Ref. [14]. At present, only limits on the D_s^{*+} width have been reported. Future experimental measurements of D_s^{*+} decays and theoretical predictions of the partial decay widths will further improve the understanding of radiative and strong decays of D_s^{*+} mesons. The world-leading precision of the BF measurement reported here will also provide improved inputs to the measurements of $f_{D_s^+}$ and $|V_{cs}|$ in $e^+e^- \to D_s^{*\pm}D_s^{\mp}$ processes.

ACKNOWLEDGMENTS

The BESIII collaboration thanks the staff of BEPCII and the IHEP computing center for their strong support. This work is supported in part by National Key R&D Program of China under Contracts No. 2020YFA0406400 and No. 2020YFA0406300; National Natural Science Foundation of China (NSFC) under Contracts No. 11635010, No. 11735014, No. 11835012, No. 11935015, No. 11935016, No. 11935018, No. 11961141012, No. 12022510, No. 12025502, No. 12035009, No. 12035013, No. 12192260, No. 12192261, No. 12192262, No. 12192263, No. 12192264, and No. 12192265; the Chinese Academy of Sciences (CAS) Large-Scale Scientific Facility Program; Joint Large-Scale Scientific Facility Funds of the NSFC and CAS under Contracts No. U1832207 and No. U1932102; 100 Talents Program of CAS; The Institute of Nuclear and Particle Physics (INPAC) and Shanghai Key Laboratory for Particle Physics and Cosmology; ERC under Contract No. 758462; European Union's Horizon 2020 research and innovation programme under Marie Sklodowska-Curie grant agreement under Contract No. 894790; German Research Foundation DFG under Contract No. 443159800, Collaborative Research Center CRC 1044, GRK 2149; Istituto Nazionale di Fisica Nucleare, Italy; Ministry of Development of Turkey under Contract No. DPT2006K-120470; National Science and Technology fund; National Science Research and Innovation Fund (NSRF) via the Program Management Unit for Human Resources & Institutional Development, Research and Innovation under Contract No. B16F640076; STFC (United Kingdom); Suranaree University of Technology (SUT), Thailand Science Research and Innovation (TSRI), and National Science Research and Innovation Fund (NSRF) under Contract No. 160355; The Royal Society, UK under Contracts No. DH140054 and No. DH160214; The Swedish Research Council; U.S. Department of Energy under Contract No. DE-FG02-05ER41374.

[1] H. Fritzsch, M. Gell Mann, and H. Leutwyler, Phys. Lett. **47B**, 365 (1973).
[2] H. Y. Cheng, C. Y. Cheung, G. L. Lin, Y. C. Lin, T. M Yan, and H. L. Yu, Phys. Rev. D **49**, 5857 (1994); **55**, 5851(E) (1997).
[3] P. Cho and M. B. Wise, Phys. Rev. D **49**, 6228 (1994).
[4] B. Wang, B. Yang, L. Meng, and S. L. Zhu, Phys. Rev. D **100**, 016019 (2019).
[5] B. Yang, B. Wang, L. Meng, and S. L. Zhu, Phys. Rev. D **101**, 054019 (2020).
[6] H. M. Choi, J. Korean Phys. Soc. **53**, 1205 (2008).
[7] J. L. Goity and W. Roberts, Phys. Rev. D **64**, 094007 (2001).
[8] T. M. Aliev, E. Iltan, and N. K. Pak, Phys. Lett. B **334**, 169 (1994).
[9] G. L. Yu, Z. Y. Li, and Z. G. Wang, Eur. Phys. J. C **75**, 243 (2015).
[10] H. B. Deng, X. L. Chen, and W. Z. Deng, Chin. Phys. C **38**, 013103 (2014).
[11] G. C. Donald, C. T. H. Davies, J. Koponen, and G. P. Lepage, Phys. Rev. Lett. **112**, 212002 (2014).
[12] A. N. Kamal and Q. P. Xu, Phys. Lett. B **284**, 421 (1992).
[13] A. Fayyazuddin and O. H. Mobarek, Phys. Rev. D **48**, 1220 (1993).

[14] C. Y. Cheung and C. W. Hwang, Eur. Phys. J. C **76**, 19 (2016).
[15] J. Gronberg *et al.* (CLEO Collaboration), Phys. Rev. Lett. **75**, 3232 (1995).
[16] B. Aubert *et al.* (*BABAR* Collaboration), Phys. Rev. D **72**, 091101 (2005).
[17] P. A. Zyla *et al.* (Particle Data Group), Prog. Theor. Exp. Phys. **2022**, 083C01 (2022).
[18] M. Ablikim *et al.* (BESIII Collaboration), Nucl. Instrum. Methods Phys. Res., Sect. A **614**, 345 (2010).
[19] C. H. Yu *et al.*, *Proceedings of IPAC2016, Busan, Korea* (JACoW, Geneva, Switzerland, 2016).
[20] M. Ablikim *et al.* (BESIII Collaboration), Chin. Phys. C **44**, 040001 (2020).
[21] K. X. Huang *et al.*, Nucl. Sci. and Tech. **33**, 142 (2022).
[22] X. Li *et al.*, Radiat. Detect. Technol. Methods **1**, 13 (2017); Y. X. Guo *et al.*, Radiat. Detect. Technol. Methods **1**, 15 (2017); P. Cao *et al.*, Nucl. Instrum. Methods Phys. Res., Sect. A **953**, 163053 (2020).
[23] M. Ablikim *et al.* (BESIII Collaboration), Chin. Phys. C **39**, 093001 (2015); **46**, 113002 (2022); These articles described the integrated luminosity measurement for data taken at $\sqrt{s} = 4.189$, 4.199, 4.209, 4.219, and 4.226 GeV. The integrated luminosity values for the other data samples have been obtained by a similar procedure.
[24] S. Agostinelli *et al.* (GEANT4 Collaboration), Nucl. Instrum. Methods Phys. Res., Sect. A **506**, 250 (2003).
[25] S. Jadach, B. F. L. Ward, and Z. Was, Phys. Rev. D **63**, 113009 (2001); Comput. Phys. Commun. **130**, 260 (2000).
[26] R. G. Ping, Chin. Phys. C **38**, 083001 (2014).
[27] D. J. Lange, Nucl. Instrum. Methods Phys. Res., Sect. A **462**, 152 (2001); R. G. Ping, Chin. Phys. C **32**, 599 (2008).
[28] J. C. Chen, G. S. Huang, X. R. Qi, D. H. Zhang, and Y. S. Zhu, Phys. Rev. D **62**, 034003 (2000); R. L. Yang, R. G. Ping, and H. Chen, Chin. Phys. Lett. **31**, 061301 (2014).
[29] E. Richter-Was, Phys. Lett. B **303**, 163 (1993).
[30] M. Ablikim *et al.* (BESIII Collaboration), Measuurement of the cross section for $e^+e^- \to D_s^{*\pm}D_s^{\mp}$ up to 4.7 GeV (to be published).
[31] N. D. Gagunashvili, Proc. Sci. ACAT2007 (**2007**) 054 [arXiv:physics/0605123].
[32] M. Ablikim *et al.* (BESIII Collaboration), Phys. Rev. D **91**, 031101 (2015).